Elastic Modulus of Polypyrrole Nanotubes

Stéphane Cuenot, Sophie Demoustier-Champagne, and Bernard Nysten*

Unité de Chimie et de Physique des Hauts Polymères, Université Catholique de Louvain, place Croix du Sud, 1, B-1348 Louvain-la-Neuve, Belgium

(Received 18 April 2000)

The first measurements of the tensile elastic modulus of polypyrrole nanotubes are presented. The nanotubes were mechanically tested in three points bending using atomic force microscopy. The elastic tensile modulus was deduced from force-curve measurements on different nanotubes with outer diameter ranging between 35 and 160 nm. It is shown that the elastic modulus strongly increases when the thickness or outer diameter of polypyrrole nanotubes decreases.

PACS numbers: 68.65.+g, 07.79.Lh, 62.20.Dc, 81.05.Lg

During the last 30 years, there was an increasing interest in the study of materials with reduced dimensions and dimensionality (2D, 1D, and 0D materials) such as thin films, nanowires, and metallic clusters. The large interest for these materials is due to the exceptional properties they can present compared to those of bulk materials (3D materials). The mechanical properties are important to determine material functionality and application domains. In the case of thin films, the most frequently investigated properties are the adhesion to the substrates, the internal residual stresses, and the tensile properties [1,2].

Recently, the developments of scanning probe microscopies enabled studies concerning nanometer-sized objects. For instance, works have been realized on carbon nanotubes such as their manipulation on various substrates and the measurement of their physical properties (elastic modulus and electrical conductivity) [3–5].

Polymer materials with low dimensionality can be prepared using different techniques. The use of track-etched membranes as templates seems to be a particularly interesting approach to synthesize polymer tubes with nanometric dimensions. Using a recently developed template-based synthesis method, nanotubes of conductive polymers can be fabricated electrochemically within the pores of polycarbonate (PC) membranes [6,7]. Using this technique, it is possible to prepare cylindrical polymer nanotubes with an outer diameter ranging from 30 to 500 nm and with a length of 20 μm. The optimized technology used to prepare PC track-etched membranes enables the fabrication of nanotubes with a very smooth surface and with a constant diameter on the entire length.

Previous studies already showed that polypyrrole (PPy) nanotubes exhibit peculiar properties [8–10]. It was observed that, when the nanotube outer diameter decreases, the electrical conductivity dramatically increases by more than 1 order of magnitude. The aim of this work is to study the effect of the reduced dimensionality on the mechanical properties of polymer nanotubes and to check if similar effects as those observed for the electrical conductivity occur. The elastic modulus of PPy nanotubes was thus measured as a function of the outer diameter using atomic force microscopy (AFM).

PPy nanotubes were electrochemically synthesized using the procedure extensively described elsewhere [6,7]. The doping agent was lithium perchlorate ($LiClO_4$). The PC membranes used as templates were 20 μm thick and had a pore density of 10^9 cm^{-2}. In order to obtain nanotubes with different outer diameters, template PC membranes with pore size ranging between 35 and 160 nm were used.

After the synthesis, the PC membrane was slowly dissolved by immersion in a dichloromethane solution with dodecyl sulfate surfactant [11]. To detach the nanotubes from the gold film previously evaporated on the backside of the membrane, the suspension was placed in an ultrasonic bath during one hour. The obtained suspensions were then filtered through poly(ethylene terephthalate) (PET) membranes with pore diameters ranging between 0.8 and 3 μm. This filtration enabled the dispersion of the nanotubes on these membranes that served afterwards as supports for the AFM measurements. In order to remove any contaminant from the nanotube surface, particularly traces of PC, the samples were again rinsed with dichloromethane.

To check that no contamination was present at the surface of the PPy nanotubes, the samples were analyzed by time-of-flight secondary ion mass spectroscopy (TOF-SIMS). For these analyses, the nanotubes were dispersed on silver membranes rather than on PET membranes, using otherwise the same procedure. The experiments were performed on a Charles Evans spectrometer using the following experimental conditions: $^{69}Ga^+$ ion beam, 15 keV acceleration voltage, 2×10^{12} ions cm^{-2} ion dose. No peak corresponding to PC was ever observed [12,13]. This ensures that the nanotubes studied by AFM were not PPy/PC composites.

The samples were also analyzed by high-resolution field effect gun scanning electron microscopy (FE-SEM) to evaluate the nanotubes dispersion on the PET membranes and to measure the inner and outer diameters of the nanotubes. The measurements performed on a large number of nanotubes allowed us to obtain a calibration curve relating the inner diameter to the outer diameter. Indeed, it was previously shown that, under identical

 0031-9007/00/85(8)/1690(4)$15.00

synthesis conditions, the same template-membrane pore diameter leads to the same nanotube thickness. This dependence is not linear and leads to a decreasing ratio between the nanotube thickness and the outer diameter with decreasing diameter. This is essentially due to the steric overall dimension of the doping anion that leads to a slower diffusion rate of the reactants in the smallest pores. For an outer diameter of 160 nm, the thickness is equal to 29 nm; it decreases under 7 nm for a diameter of 35 nm. This calibration curve was further used to estimate the inner diameter of the studied nanotubes since the AFM enabled only the measurement of the outer diameter.

The elastic modulus of the PPy nanotubes was measured with an Autoprobe® CP microscope (Thermomicroscopes, Sunnyvale, CA) operating in air with a 100 μm scanner equipped with ScanMaster® detectors correcting for nonlinearity and hysteresis effects. The cantilevers were standard Si_3N_4 Microlevers™ (pyramidal tip). For each cantilever, the spring constant was calibrated by deflecting it against a reference cantilever of known spring constant [14]. Values ranging between 0.3 and 0.5 N m^{-1} were obtained. The typical tip apex radius of curvature (around 50 nm) was expected to limit tip indentation into nanotubes because it is comparable to the nanotube radius.

The first step of the AFM analysis consisted in taking images of the sample at large scale (up to 80 $\times$ 80 μm^2) in order to visualize and to select nanotubes suspended over pores. Most of the nanotubes were lying on the membrane surface but some of them went over pores and could be used to measure their mechanical properties (Fig. 1). Once a suspended nanotube was located, an image of the nanotube at lower scale (down to 1 $\times$ 1 μm^2) was realized to precisely measure its suspended length L and its outer diameter d_{out}. The apparent nanotube width measured by AFM results from a combination of the nanotube and the tip shapes. It could not be used to estimate accurately the nanotube diameter. Therefore, nanotube outer diameter was determined by the measurement of the height. The inner diameter d_{in} was calculated using the calibration curve previously established by FE-SEM.

After selecting a nanotube crossing a hole, the AFM tip was precisely located at the midpoint along the suspended length. The nanotube was then mechanically tested in three points bending by performing force-curve measurement using the ScanMaster® detector to measure the actual sample displacement and working in the linear dynamic of the photodetector ($V_{A\text{-}B}$ around 0 V). This procedure provides curves relating the force exerted by the cantilever to the imposed sample vertical displacement z [Fig. 2(a)]. These curves were then converted into force versus nanotube deflection, δ, curves using the relation $\delta = z - d$, where d is the measured cantilever vertical deflection [Fig. 2(b)]. The reversibility (coincidence of approach and retraction curves) of the nanotube deflection and the linearity of the force-deflection curves at low forces ($F < 30$ nN) prove that the nanotube behavior is linear and elastic in this range of applied forces. The force curve measured on a portion of a nanotube lying on the membrane also shows that nanotube flattening out and tip indentation in the nanotube are negligible in the range of applied forces (Fig. 2). Indeed, in this case, the cantilever deflection is equal to the sample displacement as revealed by the infinite slope of the force-deflection curve in the contact zone.

To deduce the elastic modulus, the slope of the force-deflection curve was first determined by linear regression, giving access to the nanotube stiffness k_t. It was measured in the linear portion of the curves at low force and deflection to take into account only pure bending of the tube and to avoid possible interference of buckling or tip indentation.

In three points bending tests, the tube deflection is due both to tensile and compressive deformations and to shear deformations. To obtain the tensile modulus E from the measured force and deflection, it is necessary to minimize shear deformations. This can be done by imposing geometrical conditions to the tested system. The ratio between

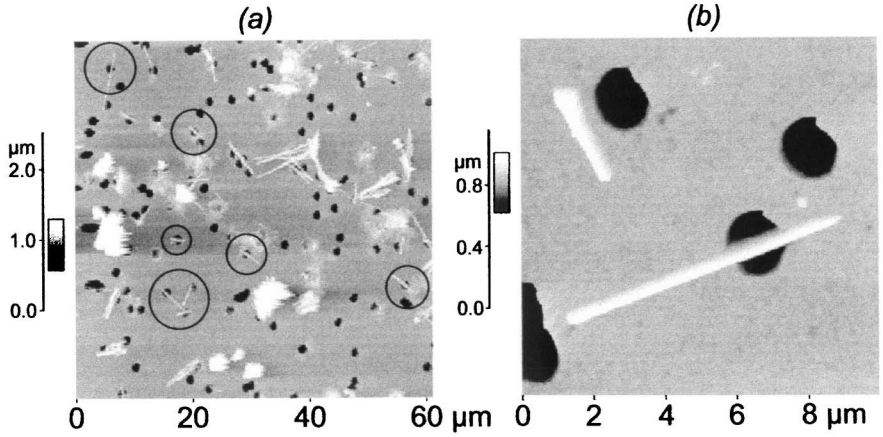

FIG. 1. (a) Large scale image of PPy nanotubes dispersed on a PET membrane revealing several tubes crossing pores (surrounded by circles). (b) Detail of a PPy nanotube suspended over a pore.

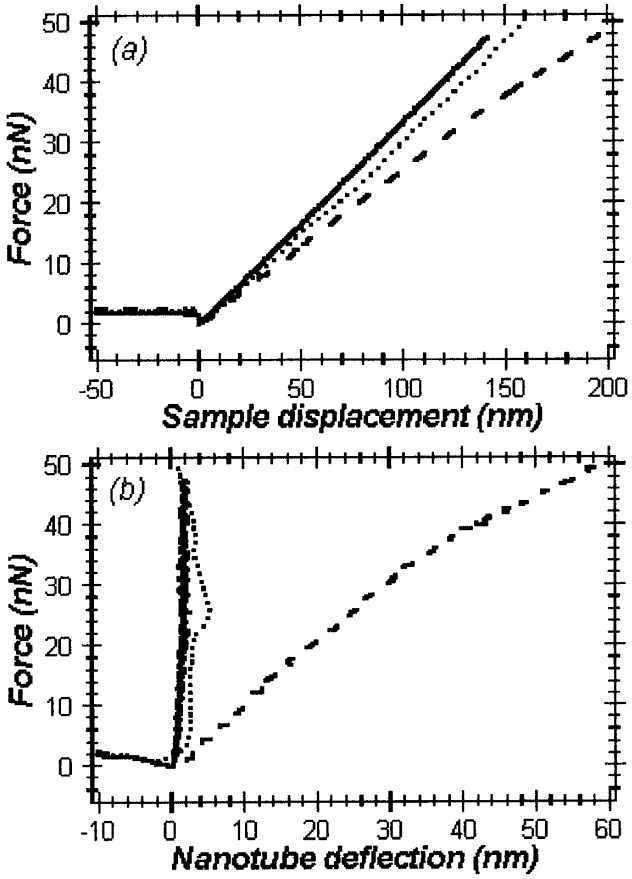

FIG. 2. (a) Typical force vs sample displacement curves obtained, respectively, on the membrane (solid line), on a nanotube located on the membrane (dotted line), and on a nanotube at the midpoint of the suspended length (dashed line). (b) Corresponding force vs nanotube deflection curves.

the suspended length of the nanotube, L, and the outer diameter d_{out} should be larger than 16 [15]. In this case, it is possible to consider that only tensile and compressive deformations are present. To achieve this, each series of nanotubes synthesized in a template membrane with a specific pore diameter was dispersed on a PET membrane with a pore diameter satisfying this criterion.

For the determination of the elastic modulus, it is necessary to know the clamping conditions of the nanotubes on the pore edges. This will indeed determine the choice of the model used to deduce the elastic modulus from the tube stiffness: supported or clamped beam. Many images were recorded with various angles between the nanotube axis and the fast scan direction as well as between the nanotube axis and the cantilever long axis due to the random dispersion of the tubes on the PET membranes. No nanotube was ever displaced during these experiments. AFM images were also recorded with stiffer cantilevers and, even in this case, no displacement was observed for the nanotube portion in contact with the membrane. The nanotube adhesion on the membrane seems thus to be sufficiently high to prevent any lift-off during the bending test. This justifies the use of the clamped-beam model to calculate the elastic modulus.

According to this model, the reduced elastic modulus E_r is given by the following relationship [15] where I is the moment of inertia of a nanotube:

$$E_r = k_t \frac{L^3}{192I} = \frac{\partial F}{\partial \delta} \frac{L^3}{192I}. \quad (1)$$

The measured elastic modulus is referred to as a reduced modulus because the above relation takes into account only pure tensile and compressive deformations. The factor 192 corresponds to the clamped-beam model.

In Fig. 3, the reduced elastic modulus is reported as a function of the outer diameter. E_r is also reported as a function of a geometrical function of the "nanotube and pore" system, $(d_{\text{out}}^4 - d_{\text{in}}^4)/L^3$. Indeed for each nanotube, three geometrical parameters are varying: the suspended length and the inner and outer diameters. On both representations, E_r increases with decreasing d_{out} or geometrical function. This ensures that the observed variation is not due to a geometrical artifact but corresponds to a variation of the intrinsic properties of the nanotube material. More precisely, the elastic modulus measured for nanotubes having a thickness higher than 20 nm, i.e., $d_{\text{out}} > 100$ nm, varies between 1.2 and 3.2 GPa. These values are comparable to those obtained for polypyrrole films [16,17]. When the nanotube thickness decreases from 20 to 16 nm ($100 > d_{\text{out}} > 70$ nm), the elastic modulus slowly increases up to 5 GPa. When the thickness decreases under 16 nm, i.e., $d_{\text{out}} < 70$ nm, the elastic modulus strongly increases with decreasing thickness or diameter. It finally reaches a value close to 60 GPa for a thickness of 6.5 nm ($d_{\text{out}} \approx 35$ nm).

The experimental error essentially arises from the uncertainty on the measurements of the geometrical parameters. Three categories of nanotubes can be defined: nanotubes with an outer diameter larger than 100 nm, those with an outer diameter between 50 and 100 nm, and those with d_{out} lower than 50 nm. On the one hand, the suspended length and the outer diameter are rather precisely measured by AFM with an accuracy of the order of 1%. On the other hand, the uncertainty on the measurements of the inner diameter is important and can be estimated to be around 15% for the smallest diameters, 6% for the intermediate diameters, and 4% for the largest diameters. The maximum uncertainty on the elastic modulus can thus be calculated to be lower than 65% for the nanotubes having their outer diameter smaller than 50 nm, 30% for those with a diameter comprised between 50 and 100 nm, and 20% for those with d_{out} larger than 100 nm. The reproducibility of the method was, in fact, tested first by measuring several force curves on the same tube. This gives the same tube stiffness value within 2%. Second, measurements were performed on series of tubes with the same diameter. The standard deviation of the determined modulus values was lower than 17% in the worst case.

The mechanical properties measured on PPy nanotubes significantly differ from those of films. The present results

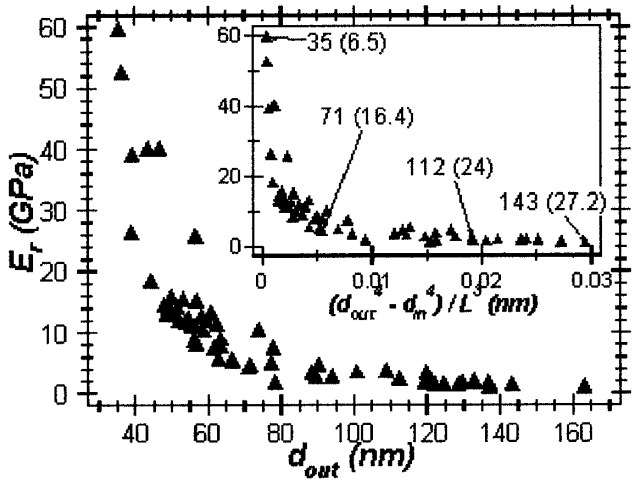

FIG. 3. Reduced elastic modulus E_r deduced from the force-curve measurements reported as a function of the nanotube outer diameter d_{out}. The inset presents E_r reported as a function of a geometrical function of the nanotube and pore system $(d_{\text{out}}^4 - d_{\text{in}}^4)/L^3$. Corresponding diameters and thicknesses (between parentheses) are reported.

indicate that the elastic modulus strongly depends on the nanotube thickness or diameter. The observed behavior for the elastic modulus is very similar to that previously observed for the electrical conductivity [7,8]. It was indeed already shown that the electrical conductivity of PPy nanotubes synthesized in the same conditions increases by more than 1 order of magnitude when the outer diameter decreases from 120 down to 35 nm.

Generally, physical properties such as the elastic modulus or the electrical conductivity are directly related to the material structural perfection. The observed variation of the modulus suggests that the degree of order of the nanotube structure increases with decreasing thickness. The observed behavior could be explained with assumptions based on the ratio of ordered chains in the nanotube. The polymer chains could be more aligned along the nanotube axis at the outer surface and could also contain less defects than the polypyrrole chains in the inner part of the nanotube.

The hypothesis concerning the reduction of defects in the polymer chains with decreasing thickness is supported by analyses using Raman spectroscopy that provides information on the relative conjugation length [7]. Raman analyses were realized on PPy nanotubes of different diameters. The ratio between the intensity of a band sensitive to the PPy oxidation state (band at 1595 cm^{-1}) and the intensity of the skeletal band (band at 1500 cm^{-1}) provides a relative measurement of the conjugation length. An increase of the π-conjugation length, normally correlated to a decrease of chain defects, was observed with the decrease of the nanotube diameter.

The better alignment of the PPy chains at the surface could be due to the fact that the pore surface of the PC membrane is negatively charged. Since PPy polymerization is oxidative, electrostatic interactions could favor the growth of the polymer chains along the tube axis. This orientation effect is more important for nanotubes with smaller thickness because the surface to volume ratio increases when the thickness decreases. Therefore, when the nanotube thickness decreases, i.e., when the outer diameter decreases, the fraction of well-ordered PPy chains increases. The elastic modulus and the electrical conductivity should increase as it is observed. In the future, studies will be realized in order to finely characterize the structure of the PPy nanotubes and to reveal chain orientation effects.

The authors gratefully acknowledge Dr. C. Fretigny (ESPCI, Paris) and Dr. J.-P. Aimé (Université Bordeaux I) for fruitful discussions and L. Rouxhet (PCPM, UCL) and C. Poleunis (PCPM, UCL) for the help with the TOF-SIMS analyses. S. C. is financially supported by the Special Funds for Research (F.S.R.) of the Université Catholique de Louvain (UCL). B. N. and S. D. C. are Research Associates of the Belgian National Funds for Scientific Research (F.N.R.S.)

*To whom correspondence should be addressed.
Electronic address: nysten@poly.ucl.ac.be

[1] R. P. Vinci and J. J. Vlassak, Annu. Rev. Mater. Sci. **26**, 431 (1996).
[2] R. W. Hoffman, in *Physics of Thin Films,* edited by G. Hass and R. E. Thun (Academic Press, New York, 1966), Vol. 3.
[3] T. Hertel, R. Martel, and P. Avouris, J. Phys. Chem. B **102**, 910 (1998).
[4] U. Hubler, P. Jess, H. P. Lang, H.-J. Güntherodt, J. P. Salvetat, and L. Forro, Carbon **36**, 697 (1998).
[5] J. P. Salvetat *et al.,* Adv. Mater. **11**, 161 (1999).
[6] S. Demoustier-Champagne, E. Ferain, R. Legras, C. Jérôme, and R. Jérôme, Eur. Polym. J. **34**, 1767 (1998).
[7] S. Demoustier-Champagne and P.-Y. Stavaux, Chem. Mater. **11**, 829 (1999).
[8] J. Duchet, R. Legras, and S. Demoustier-Champagne, Synth. Met. **98**, 113 (1998).
[9] S. Demoustier-Champagne, J. Duchet, and R. Legras, Synth. Met. **101**, 20 (1999).
[10] V. P. Menon, J. Lei, and C. R. Martin, Chem. Mater. **8**, 2382 (1996).
[11] S. De Vito and C. R. Martin, Chem. Mater. **10**, 1738 (1998).
[12] D. Briggs, A. Brown, and J. C. Vickerman, *Handbook of Static Secondary Ion Mass Spectrometry (SIMS)* (Wiley, Chichester, 1989).
[13] M. L. Abel, S. R. Leadley, A. M. Brown, J. Petitjean, M. M. Chehimi, and J. F. Watts, Synth. Met. **66**, 85 (1994).
[14] M. Tortonese and M. Kirk, *Micromachining and Imaging,* SPIE Proceedings Vol. 3009 (SPIE–International Society for Optical Engineering, Bellingham, WA, 1997), p. 53.
[15] S. P. Timoshenko and J. M. Gere, *Mechanics of Materials* (Van Nostrand, New York, 1972).
[16] M. Gandhi, G. M. Spinks, R. P. Burford, and G. G. Wallace, Polymer **36**, 4761 (1995).
[17] B. Sun, J. J. Jones, R. P. Burford, and M. Skyllas-Kazacos, J. Mater. Sci. **24**, 4024 (1989).